separations

MDPI

Article

Efficient Separation of Re (VII) and Mo (VI) by Extraction Using E-1006–Ammonium Sulfate Aqueous Two-Phase System

Linlin Fan, Wenhui Li, Zilong Dai, Min Zhou and Yunren Qiu *

School of Chemistry and Chemical Engineering, Central South University, Changsha 410083, China; fanlinlin0508@163.com (L.F.); liwenhui@163.com (W.L.); csudaizilong12152@163.com (Z.D.); zhouminnn@126.com (M.Z.)

* Correspondence: csu_tian@csu.edu.cn

Abstract: Aqueous two-phase extraction (APTE) stands out as an environmentally friendly technique for the separation of metal ions. The separation of Re (VII) and Mo (VI) in an aqueous solution was investigated using a novel aqueous two-phase system (ATPS) consisting of isodecanol polyoxyethylene ether (E-1006), ammonium sulfate, and water. A phase diagram of this system was developed, and the effects of pH, temperature, extraction time, the concentrations of E-1006 and $(NH_4)_2SO_4$, and metal ions on the separation of Re (VII) and Mo (VI) were examined. The results show that at pH 7.0, Mo (VI) had almost transformed into the $(NH_4)_2SO_4$-rich phase, while Re (VI) was extracted into the E-1006-rich phase. The increase in temperature induces a transition of Mo (VI) to the salt-rich phase, which is unfavorable for the extraction of Re (VII). The increase in the concentrations of E-1006 and $(NH_4)_2SO_4$ has a positive effect on the separation of rhenium and molybdenum. Overall, the ATPS consisting of 200 g/L of E-1006, 200 g/L of $(NH_4)_2SO_4$, and water yields an extraction efficiency of 97.2% for Re and a high separation factor of 2700 for Re (VII) and Mo (VI) from a mixture of 0.1 g/L of Re (VII) and 5 g/L of Mo (VI) at pH 7.0 and 323.15 K. Separation studies of the simulated leaching solution show that the extraction efficiency for Re (VI) is 99.1% and the separation factor of Re (VII) and Mo (VI) is 5100.

Keywords: aqueous two-phase system; phase equilibrium; rhenium-molybdenum separation; E-1006

Citation: Fan, L.; Li, W.; Dai, Z.; Zhou, M.; Qiu, Y. Efficient Separation of Re (VII) and Mo (VI) by Extraction Using E-1006–Ammonium Sulfate Aqueous Two-Phase System. *Separations* **2024**, *11*, 142. https://doi.org/10.3390/separations11050142

Academic Editor: Gavino Sanna

Received: 1 March 2024
Revised: 29 April 2024
Accepted: 30 April 2024
Published: 7 May 2024

1. Introduction

Molybdenum has excellent electrical and thermal conductivity and a melting point of up to 2620 °C [1], and it can be used as an important alloy additive [2], significantly improving the toughness and high-temperature strength of a material. Rhenium is an ultra-high-melting-point metal with a melting point of up to 3180 °C. Rhenium also has excellent stability, high-temperature elasticity, and ductility. The production of high-performance alloys, nanomaterials, and catalysts cannot be achieved without the addition of rhenium. In addition, molybdenum and rhenium are important raw materials for aerospace and national development [3].

Due to the similar ionic radii of Re^{4+} and Mo^{4+}, rhenium usually exists in the form of analogs in sulfide deposits such as molybdenite and copper ores. The rhenium content in molybdenite is relatively high and has a certain economic recovery value. Therefore, the separation and enrichment of molybdenum and rhenium in the leaching solution of molybdenite after ammonia leaching treatment is the key to obtaining rhenium and molybdenum resources. Currently, there are many methods for separating rhenium and molybdenum from a leaching solution, such as solvent extraction [4,5], ion exchange [6–8], and membrane separation [9–11]. Due to its advantages in terms of easily operable equipment and high selectivity, solvent extraction technology [2,5,12] stands out as the most widely used tool for this application. Commonly used extractants in the hydrometallurgical industry with respect to rhenium and molybdenum include organophosphorus extractants,

as well as amine extractants, such as TBP, P204, Cyanex 27 [13], TOA, N263, etc. Aifei Yi et al. [4] studied the extraction and separation of rhenium and molybdenum from the alkaline leaching solution of a waste-based high-temperature alloy using N263 as the extractant, and the extraction efficiency for Re reached 99% when O/A was 1/30 and under the first extraction condition. In the extraction of rhenium from acid chloride solutions using Cyanex 923, the extraction efficiency for Re can reach 99.2% [14]. Alamine 336 and TBP were used to synergistically extract perrhenate from an industrial leaching solution, in which the leaching solution was an acidic leaching solution of sulfuric acid and ammonium persulfate, and the separation efficiency for perrhenate reached more than 99.90% after a four-stage countercurrent extraction [15]. Solvent extraction has achieved good results in the separation and enrichment of rhenium and molybdenum. However, the traditionally used solvent extraction solution leads to the loss of organic solvents, environmental pollution, and adverse effects on human health.

Aqueous two-phase extraction (ATPE) is a promising alternative to hydrometallurgical processes for the selective extraction of metals since it does not involve organic solvents and is simple to perform. In ATPE, the differences in solute partition coefficients between the two phases caused by salting-out, intermolecular spatial hindrance, and external environments are used to achieve the selective separation of solutes. The hydrophobicity of polymers formed by an aqueous two-phase system (ATPS) enhances the interaction of the alkali component with the polymer phase. In the same way, the salting-out effect can further distinguish the phases, which may favor the distribution of the solute to the phase of greater affinity [16]. This method has been successfully studied for the extraction of Mo [17], the separation of molybdenum and vanadium [18], and the separation of other ions [19]. Li Ruisi et al. [20] used an ATPS consisting of the nonionic surfactant Triton X-100 and Na_2SO_4 to investigate the extraction separation effect of tungsten and molybdenum in an aqueous solution when no extractant was added, and the separation factor of tungsten and molybdenum was up to 328 at a pH 2.0, 343.15 K, and a mass fraction of sodium tartrate as a complexing agent of 3%. Daniela da Silveira Leited et al. [21] investigated the selective extraction of copper and cobalt from spent lithium-ion batteries via ATPS, and the optimal conditions resulted in a separation coefficient of 3.22×10^2 for copper and cobalt. However, little work has been reported for the separation of rhenium and molybdenum via ATPS.

A novel ATPS consisting of isodecanol polyoxyethylene ether (E-1006), ammonium sulfate, and water was constructed and applied for the separation of Re (VII) and Mo (VI). The effects of pH, temperature, extraction time, E-1006 concentration, ammonium sulfate concentration, and metal ion concentrations on the separation of Re (VII) and Mo (VI) were investigated to explore the optimal process conditions for the separation of Re (VII) and Mo (VI) from acidic solutions. This research can guide the separation of Re and Mo in the industry.

2. Materials and Methods

2.1. Materials and Apparatus

The commercial nonionic surfactant $(C_2H_4O)_nC_{10}H_{22}O$ (E-1006), with an average hydroxyl value of 132 (130–134), and ammonium perrhenate (NH_4ReO_4) with a purity of 0.99 (mass fraction, same as below) were purchased from Shanghai McLean Technology Biochemistry Co., Ltd. (Shanghai, China). The chemical structure of E-1006 is shown in Figure 1. Ammonium sulfate ($(NH_4)_2SO_4$) with a purity of 0.99 and ammonia solution (NH_4 OH) with a purity of 0.25–0.28 were supplied by China National Pharmaceutical Group Chemical Reagent Co., Ltd. (Shanghai, China). Ammonium molybdate tetrahydrate ($(NH_4)_6Mo_7O_{24}{\cdot}4H_2O$) with a purity > 0.99 and sulfuric acid (H_2SO_4) with a purity of 0.95–0.97 were provided by Chengdu Kelong Chemical Co., Ltd. (Chengdu, China). Either NH_4OH and H_2SO_4 were used to adjust the pH of aqueous solutions. The inorganic chemicals used were of analytical grade. All the water used in the experiment was deionized water.

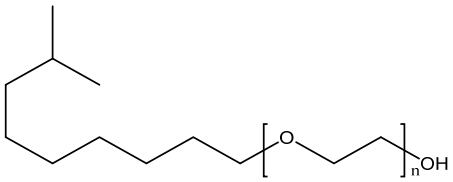

Figure 1. E-1006 chemical structural formula.

An analytical balance (AUY220, SHIMADZU, Kyoto, Japan) was used for weighting the reagents. The pH and conductivity measurements were carried out with a pH meter (PHS-3C, Shanghai Leici Instrument Co., Ltd., Shanghai, China) and a conductometer (DDS-307, Shanghai Leici Instrument Co., Ltd., Shanghai, China), respectively. A constant-temperature-heating magnetic stirrer (DF-101S, Gongyi Chuangyuan Instrument Manufacturing Co., Ltd., Zhengzhou, China) was used to stir the mixture of Re-Mo solution and ATPS. Then, phase separation was achieved via heating separation in a digital-display-equipped constant-temperature water bath pot (WB100-6, Qun'an Instrument Co., Ltd., Huzho, China). The concentrations of Re (VII) and Mo (VI) were quantified using Inductively Coupled Plasma Optical Emission Spectrometry (ICP-OES, ThermoFisher USA, Inc., Waltham, MA, USA, U.S.ICAP 6300 Radial, for which the RF power was 1300 W; the flux of auxiliary air was 0.2 L·min^{-1}; the flux of carrying air was 0.7 L·min^{-1}; the pump speed was 1.0 r·min^{-1}; and the method of observing plasma was automatic). Fourier transform infrared spectrometry (FTIR, PerkinElmmer company, Waltham, MA, USA) was employed to analyze the changes in the chemical structure and functional groups of E-1006. The change in particle size of the E-1006-rich phase was determined using the Nano ZS90 dynamic light-scattering instrument (DLS, Malvern Instruments, Malvern, UK).

2.2. Experimental Methods

2.2.1. Phase Diagram of the ATPS

Liquid–liquid equilibrium data were obtained for an ATPS consisting of different concentrations of aqueous solutions of E-1006 and $(NH_4)_2SO_4$. The bimodal curve, which divides a region of component concentrations that will form two immiscible aqueous phases, was obtained using the gravimetric method. At a certain temperature, a 40 g solution mixture was vigorously stirred in a magnetic stirrer for 30 min and then deposited in a thermostatic bath with a graduated test tube for 10 h. Samples of the top and bottom phases were collected to determine the mass fractions of E-1006 and $(NH_4)_2SO_4$.

The concentration of $(NH_4)_2SO_4$ was determined by measuring conductivity within a linear range of $(NH_4)_2SO_4$ concentrations; further, we obtained the mass fraction of $(NH_4)_2SO_4$, for which the conductivity of the salt solutions was independent of the polymer composition. The mass fraction of water was calculated based on the water lost from the oven-dried specimen, and then the mass fraction of E-1006 was obtained. Utilizing the obtained data, a phase diagram was constructed, with the mass fraction of $(NH_4)_2SO_4$ on the horizontal axis and the mass fraction of E-1006 on the vertical axis.

2.2.2. Re-Mo Separation

The separation of Re (VII) and Mo (VI) in ATPS was investigated as a function of pH (1.0 to 7.0), temperature (303.15 K to 333.15 K), concentrations of E-1006 ($c_{E\text{-}1006}$) and $(NH_4)_2SO_4$ ($c_{(NH4)SO4}$) (50 g/L to 200 g/L), Re (VII) concentration (c_{Re}) (0.01 g/L to 0.1 g/L), and Mo (VI) concentration (c_{Mo}) (2 g/L to 10 g/L). Stock solutions of $(NH_4)_2SO_4$, Re (VII), and Mo (VI) were prepared using ammonium sulfate, ammonium perrhenate, and ammonium molybdate tetrahydrate, respectively.

For the extraction experiment, volumes of $(NH_4)_2SO_4$, Re (VII), and Mo (VI) stock solutions were mixed, adding a certain amount of deionized water and E-1006 to achieve a total volume of 40 mL. The pH of the solution was adjusted by adding the required amount of sulfuric acid and ammonia solution. At a certain temperature, the beaker containing the solution mixture was vigorously stirred in a magnetic stirrer for 20 min and placed in a

thermostatic bath with a graduated test tube for 2 h. The scheme of the Re-Mo separation is shown in Figure 2. The volumes of the top and bottom phases were recorded, and samples of the $(NH_4)_2SO_4$-rich phase were collected. The samples were diluted for measuring the c_{Re} and c_{Mo} via ICP-OES.

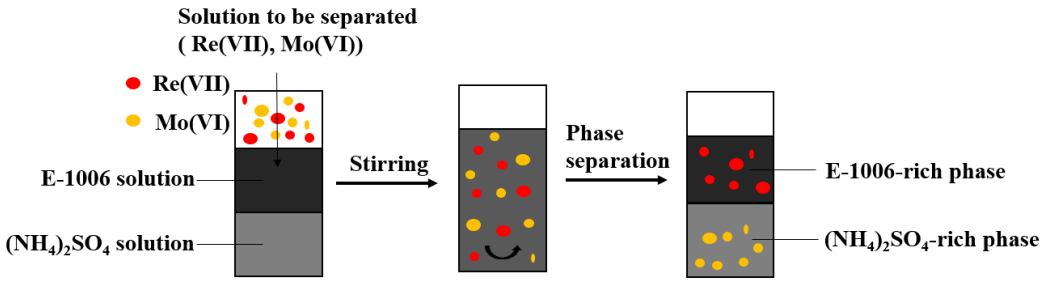

Figure 2. Scheme of Re (VII) and Mo (VI) separation.

The concentration of metal ions in the E-1006-rich phase, the distribution coefficient (D) and extraction efficiency (E) in the E-1006 phase, and the separation factor (S) of the aqueous two-phase extraction process are defined as follows:

$$c_1 = \frac{m - V_2 c_2}{V_1} \quad (1)$$

$$D = \frac{c_1}{c_2} \quad (2)$$

$$E = \frac{c_1 V_1}{m} \times 100\% \quad (3)$$

$$S_{Re/Mo} = \frac{D_{Mo}}{D_{Re}} \quad (4)$$

where c_1 and c_2 represent the concentrations of metal ions in the E-1006-rich aqueous phase and the $(NH_4)_2SO_4$-rich aqueous phase, respectively. V_1 and V_2 are the respective volumes of the E-1006-rich aqueous phase and the $(NH_4)_2SO_4$-rich aqueous phase. m represents the mass of metal ions added to the system.

3. Results and Discussion

3.1. Phase Diagrams

The ternary mixtures of surfactant, salt, and water, upon reaching thermodynamic equilibrium, cause exclusion among the components, resulting in the formation of two phases. Phase diagrams can explain the solute separation behavior of ATPS during the extraction process. A phase diagram of the ATPS formed by E-1006 and $(NH_4)_2SO_4$ at 313.15 K is shown in Figure 3. The good water solubility of E-1006 is mainly dependent on the hydrogen atoms in the water molecules connecting with the C–O–C groups on E-1006 to form hydrogen bonds and rapidly fuse with water [22]. The salting-out action of $(NH_4)_2SO_4$ breaks the above hydrogen bonds, leading to the dehydration of E-1006 [23]. In an ATPS, the content of E-1006 and $(NH_4)_2SO_4$ increases, that of the binodal curve is closer to the x-axis, and the tie-line length is longer, indicating a stronger ability for phase separation.

Temperature is an important factor affecting phase separation in ATPSs [24]. In this study, we investigated the phase equilibria of the ATPS in question at temperatures of 303.15 K, 313.15 K, and 323.15 K. The results are shown in Figure 4 and Supplementary, where it is shown that an increase in the temperature promotes an increase in larger biphasic regions [25]. This phenomenon can be explained by the enhanced irregular thermal motion of the molecules, the breakage of the hydrogen bonds between E-1006 and water molecules, and the decrease in the solubility of E-1006 in water, leading to an increase in the content of E-1006 in the upper phase and an increase in the content of salt in the lower phase. The area of the biphasic region increased, indicating that the increase in temperature promotes phase separation.

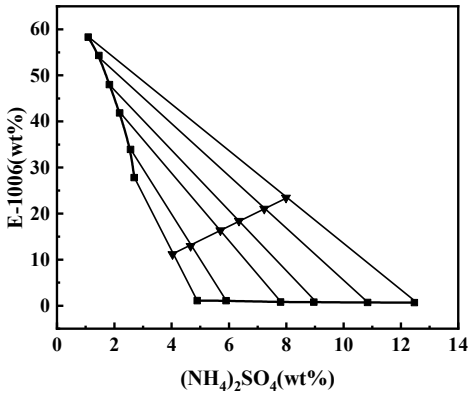

Figure 3. Phase diagram of ATPS composed of E-1006 and $(NH_4)_2SO_4$ at 313.15 K.

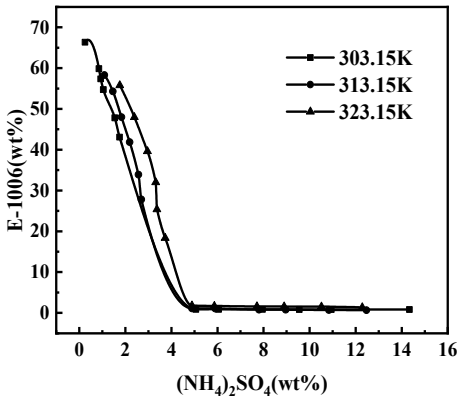

Figure 4. Phase diagram of ATPS composed of E-1006 and $(NH_4)_2SO_4$ at different temperatures.

3.2. The Separation of Re (VII) and Mo (VI)

3.2.1. Effect of pH

The morphology of Re (VII) and Mo (VI) present in solution varies considerably at different pH levels, as does the water solubility of the ions. The distribution of Re (VII) and Mo (VI) in this system is significantly influenced by pH. The separation of Re (VII) and Mo (VI) was studied at different pH levels using an ATPS consisting of 100 g/L of E-1006 and 100 g/L of $(NH_4)_2SO_4$, and the feed consisted of 0.1 g/L of Re (VII) and 5 g/L of Mo (VI). The temperature was maintained at 313.15 K. Figure 5 shows the variation in E_{Re}, E_{Mo}, and the $S_{Re/Mo}$ with respect to pH from 1.0 to 7.0. One can see that the E_{Re} increases from 71.44% to 83.60% as the pH increases from 1.0 to 2.0. A further increase in pH to 7.0 results in a slight increase in E_{Re}. On the other hand, the E_{Mo} reaches a maximum at pH 2.0, and most of the Mo (VI) is distributed in the $(NH_4)_2SO_4$-rich phase at pH 7.0. The $S_{Re/Mo}$ is very low at higher acidity levels, but it experiences a great increase as pH rises, reaching a maximum value of 129.67 at pH 7.0.

Accompanied by the formation of the ATPS, the system was divided into a hydrophobic phase, where E-1006 is located, and a hydrophilic phase, where $(NH_4)_2SO_4$ is located. The Fourier Transform Infrared Spectroscopy (FTIR) analysis results (Figure 6) show that the characteristic absorption peak at a wavenumber of 1100 cm^{-1} corresponds to the ether bond (C–O–C) in the molecular structure of E-1006 [26]. The position of this peak is 1100 cm^{-1} in pure E-1006 and 1099 cm^{-1} in E-1006 at pH 7.0. There is no obvious shift, which suggests that the addition of ammonia does not significantly affect the vibration of the ether bond. Noteworthily, the absorption peak of the ether bond is 1091 cm^{-1} after the separation of Re (VII) and Mo (VI). The slight redshift of the characteristic peak of C–O–C after extraction suggests the presence of a specific force between the E-1006 molecule and Re (VII) during the extraction process. The characteristic absorption peaks at 2860–3000 cm^{-1} were attributed to the C–H bond [27]. The significant change in the C–H characteristic

absorption peaks after the extraction of Re (VII) can be attributed to the alteration of the environment surrounding the C–H bond in the E-1006 molecule, resulting in a shift in its vibrational state. In addition, the broad peak at 3000–3800 cm^{-1} represents the absorption peak of the hydroxyl group (–OH) [28]. The curves in Figure 6a,b demonstrate that the weak absorption peaks in this region for pure E-1006 and E-1006 at pH 7.0 correspond to the presence of hydroxyl groups in the molecular structure of E-1006. Corresponding to the period after the extraction of Re (VII), the curve in Figure 6c shows that the absorption peak of –OH in the E-1006-rich phase is significantly enhanced and encompasses lower wavenumbers. This indicates the presence of a hydrogen-bonding network, possibly due to the presence of specific water molecules in the E-1006-rich phase after the extraction. Meanwhile, the curve in Figure 6c shows a significant enhancement of the –OH bending vibrational peak at ~1600 cm^{-1} compared with that in Figure 6a,b, which also supports this conclusion.

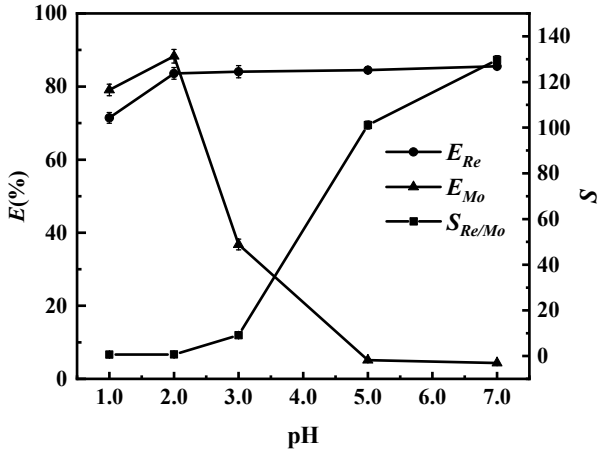

Figure 5. Effect of pH on the E_{Re}, E_{Mo}, and $S_{Re/Mo}$.

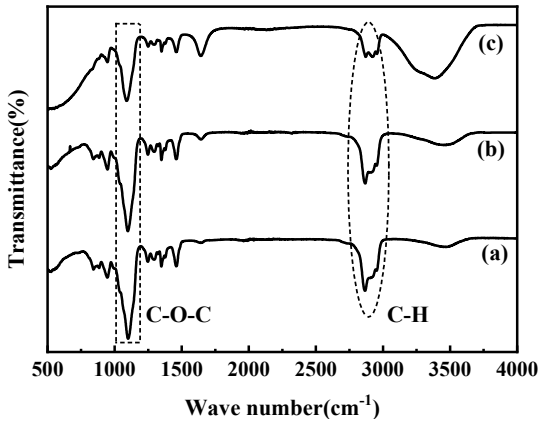

Figure 6. FTIR spectra of Re-Mo separated by the studied ATPS consisting of E-1006, $(NH_4)_2SO_4$, and H_2O. (**a**), pure E-1006; (**b**), E-1006 aqueous solution at pH 7.0; (**c**), E-1006-rich phase after Re-Mo separation at pH 7.0.

According to the distribution diagram of Re (VII) [14], Re (VII) primarily exists as ReO_4^- with strong hydrophobicity [29] in the pH range of 0–13. The forms of Mo (VI), along with the calculated ratios of charge, mass, and charge density at different pH levels, are shown in Table 1 [30]. |z| denotes the absolute value of ion charge, n is the atomic number of an ion, and M is molar mass. |z|/M is charge density. At pH $\geq$ 7.0, Mo exists mainly in the form of MoO_4^{2-}, which has a relatively large value of charge density, that is, 0.0125, and a higher hydrophilicity. Importantly, at pH 7.0, the hydrophobicity of ReO_4^- is

responsible for the extraction into the E-1006 phase, and MoO_4^{2-} remains in the salt-rich phase due to its hydrophilicity, realizing an efficient separation of Re (VII) and Mo (VI).

Table 1. The ratio of charge, mass, and charge density of Mo (VI) at different pH levels.

pH	<1.8	<2.5	<4	<5	<7	>7
Species	MoO_2^{2+}	$H_2Mo_7O_{24}^{4-}$	$HMo_7O_{24}^{5-}$	$Mo_7O_{24}^{6-}$	$Mo_2O_7^{2-}$	MoO_4^{2-}
|z|/n	0.6667	0.1212	0.1562	0.1935	0.2222	0.4000
|z|/M	0.01562	0.003774	0.004726	0.005682	0.006579	0.01250

Therefore, the initial pH of the solution should be adjusted to 7.0 first for the APTE of Re (VII) and Mo (VI). The pH in the subsequent experiments was set to 7.0.

3.2.2. Effect of Temperature

In the exploration of ATPS phase equilibrium, temperature is closely related to phase separation. The effect of temperature, ranging from 303.15 to 333.15 K, on the E_{Re}, E_{Mo}, and $S_{Re/Mo}$ is shown in Figure 7.

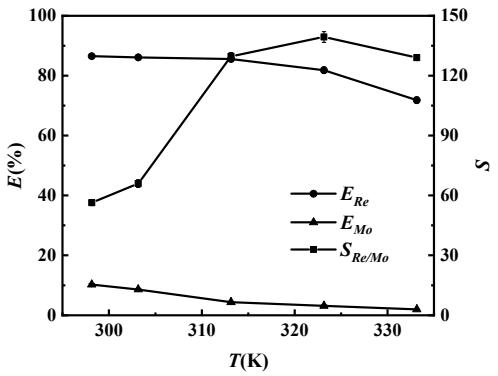

Figure 7. Effect of temperature on the E_{Re}, E_{Mo}, and $S_{Re/Mo}$.

Both E_{Re} and E_{Mo} decrease with temperature. The E_{Re} is favored at low temperatures, as demonstrated by the E_{Re} at 298.15 K that is close to 87%. The increase in temperature promotes the transfer of the more-hydrophilic MoO_4^{2-} to the $(NH_4)_2SO_4$-rich phase. The $S_{Re/Mo}$ shows a tendency to increase and then decrease, with a peak value of 139.37 at 323.15 K [31].

3.2.3. Effect of $c_{E\text{-}1006}$

$c_{E\text{-}1006}$ affects the number of micelles formed in an ATPS and plays a crucial role in the separation effect of metal ions. To study the effect of $c_{E\text{-}1006}$ on the separation of Re (VII) and Mo (VI), ATPSs composed of different concentrations of E-1006 in the range of 50 g/L to 200 g/L were prepared and mixed with 100 g/L of $(NH_4)_2SO_4$ at pH 7.0 and 313.15 K, as depicted in Figure 8.

With the increase in $c_{E\text{-}1006}$ from 50 g/L to 200 g/L, the E_{Re} increases from 60.71% to 93.66%, and the $S_{Re/Mo}$ increases from 25.03 to 514.24, which can be attributed to the greater number of micelles colliding with each other, prompting more ReO_4^- to be solubilized into the micelles of the E-1006 phase [30]. The increase in micelles makes the E-1006 phase more hydrophobic and promotes the transformation of MoO_4^{2-} into the salt-rich phase [32]. While an increase in $c_{E\text{-}1006}$ generally favors the separation of Re (VII) and Mo (VI), it is essential to consider the drawbacks of excessive concentrations. High concentrations can lead to emulsification of the solution, posing challenges for subsequent treatment processes. The suitable $c_{E\text{-}1006}$ was determined to be 200 g/L, taking into account the favorable $S_{Re/Mo}$ and the economic cost of the agent.

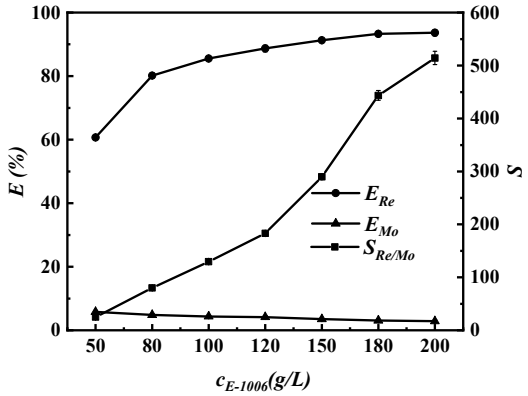

Figure 8. Effect of $c_{E\text{-}1006}$ on the E_{Re}, E_{Mo}, and $S_{Re/Mo}$.

The changes in particle size and zeta potential of the E-1006-rich phase were analyzed using dynamic light scattering (DLS) to speculate on the possible mechanism of the transition of Re (VII) into the E-1006-rich phase [33,34]. Figure 9 shows a micelle size analysis of the E-1006 phase, where the two lines are the micelle sizes in the aqueous solution of E-1006 and the aqueous solution of the E-1006 phase after Re (VII) extraction, respectively. The particles of the E-1006 micellar phase after Re (VII) extraction are larger. Table 2 shows the potential change of the E-1006 phase. Sample 1 is the E-1006 aqueous solution, sample 2 is the E-1006 aqueous solution at pH 7.0, and sample 3 is the E-1006 aqueous solution after Re-Mo separation at pH 7.0. The average zeta potential of the E-1006 micellar phase (0.110 mV) is slightly positive at pH 7.0 and becomes negative (−1.23 mV) after Re (VII) extraction, which can be attributed to ReO_4^- diffusing into the hydrophobic environment inside the E-1006 micelles due to its strong hydrophobicity [14,20].

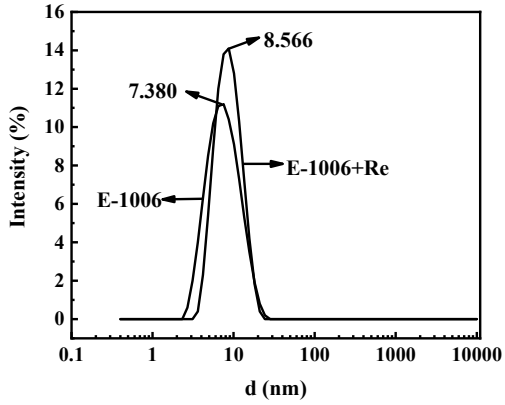

Figure 9. Particle size analysis of micelles in the E-1006 phase.

Table 2. Potential changes in the micellar phase of E-1006.

Sample Number	Zeta Potential (mV)
1	−0.642
2	0.110
3	−1.230

3.2.4. Effect of $c_{(NH4)SO4}$

Under specific conditions involving the addition of inorganic salts, the E-1006 aqueous solution undergoes phase separation [35]. However, at low salt concentrations, the experimental system fails to form distinct phases. On the premise of ensuring the formation of different phases, the addition of $(NH_4)_2SO_4$ was explored, ranging from 50 g/L to 200 g/L.

Figure 10 presents the effect of $c_{(NH4)SO4}$ on the separation of Re (VII) and Mo (VI), indicating that $c_{(NH4)SO4}$ has an important influence on the separation of Re (VII) and Mo (VI).

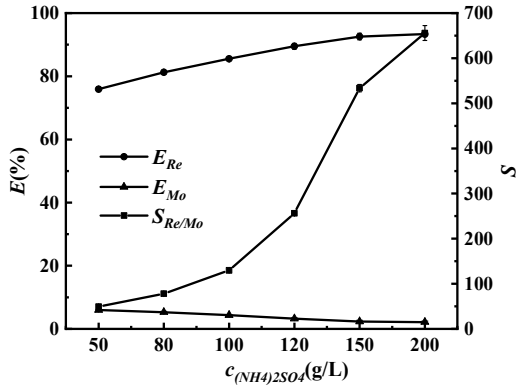

Figure 10. Effect of $c_{(NH4)SO4}$ on the E_{Re}, E_{Mo}, and $S_{Re/Mo}$.

As shown in Figure 10, as the amount of $c_{(NH4)SO4}$ increases from 50 g/L to 200 g/L, the E_{Re} increases from 75.92% to 93.39%, and the $S_{Re/Mo}$ rises from 49.35 to 655.90. $(NH_4)_2SO_4$ is a kosmotropic salt, and its free energy of hydration is large (in terms of the absolute value) [32]. Its salting-out ability is strong and becomes stronger with an increasing concentration, which results in a decreasing free water concentration, creating a more chaotropic polymolybdate anion dehydrate and increasing the number of micellar aggregates [36]. The difference in hydrophilicity between the two phases is larger, promoting the transition of ReO_4^- to the E-1006-rich phase, while MoO_4^{2-} is more prone to transition to the $(NH_4)_2SO_4$-rich phase. The selection of 200 g/L $c_{(NH4)SO4}$ is a suitable condition for the effective separation of Re (VII) and Mo (VI).

3.2.5. Effect of c_{Re} and c_{Mo}

The effects of c_{Re}, ranging from 0.01 g/L to 0.1 g/L, and c_{Mo}, ranging from 2 g/L to 10 g/L, on the separation of Re (VII) and Mo (VI) were investigated. To specifically assess the influence of the initial c_{Mo}, the c_{Re} was maintained at 0.1 g/L, while for studying the impact of the initial c_{Re}, c_{Mo} was held constant at 5 g/L. The obtained results are shown in Figure 11 and Figure 12, respectively.

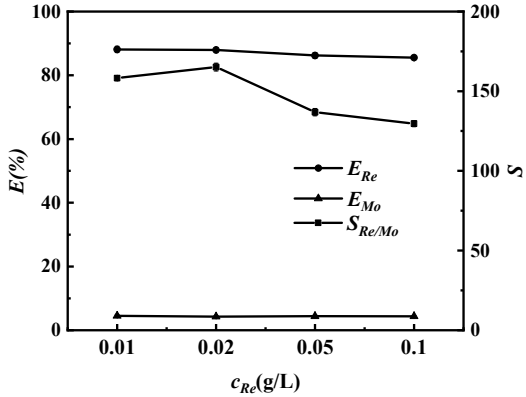

Figure 11. Effect of c_{Re} on the E_{Re}, E_{Mo}, and $S_{Re/Mo}$.

Figure 11 shows that an increase in c_{Re} has a negligible effect on E_{Re}, while E_{Re} tends to decrease. $S_{Re/Mo}$ decreases as c_{Re} increases. Figure 12 shows the effect of the initial c_{Mo} on the separation of Re (VII) and Mo (VI). It is clear that c_{Mo} has a negligible effect on E_{Mo}, but E_{Re} increases with an increasing Mo (VI) concentration. At pH 7.0, MoO_4^{2-} is highly hydrophilic, and the increase in the Mo (VI) concentration has a promoting effect on the transition of ReO_4^- to the hydrophobic phase.

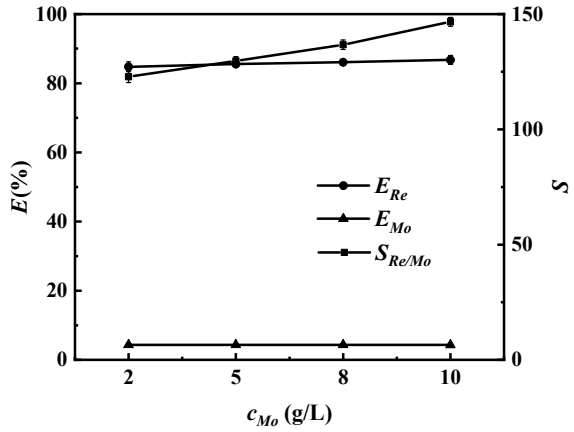

Figure 12. Effect of c_{Mo} on the E_{Re}, E_{Mo}, and $S_{Re/Mo}$.

3.2.6. Effect of Extraction Time

The extraction time greatly affects the extraction and separation of ions. In this section, the results of the separation of Re (VII) and Mo (VI) in the ATPS are investigated at an extraction time ranging from 15 min to 10 h. The results are shown in Figure 13.

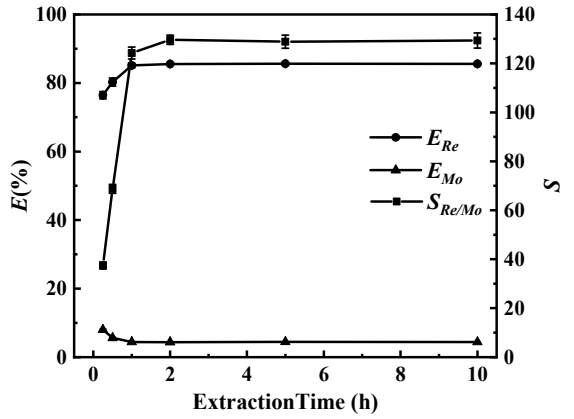

Figure 13. Effect of extraction time on the E_{Re}, E_{Mo}, and $S_{Re/Mo}$.

As can be seen in Figure 13, the extraction efficiencies and the separation factor of Re (VII) and Mo (VI) in the E-1006-rich phase increase significantly in the range of 15 min to 2 h and increase very little from 2 h to 10 h. The Re (VII) transitions to the E-1006-rich phase, and Mo (VI) transitions to the $(NH_4)_2SO_4$-rich phase. The extraction tends to equilibrate at 2 h, and the separation factor of rhenium and molybdenum tends to stabilize. Thus, 2 h is suitable for separation.

3.3. Separation of Re (VII) and Mo (VI) under Suitable Conditions

Based on the insights gained from the factors affecting the separation of Re (VII) and Mo (VI), the separation result of the solution containing 0.1 g/L of Re (VII) and 5 g/L of Mo (VI) under suitable conditions is outlined in Table 3. It indicated that E_{Re} reached 97.2%, and the $S_{Re/Mo}$ was 2700.

Table 3. Suitable conditions for separation behavior.

$c_{E\text{-}1006}$/ g L^{-1}	$c_{(NH4)2SO4}$/ g L^{-1}	pH	Temperature/ K	E_{Re}/%	E_{Mo}/%	$S_{Re/Mo}$
200	200	7.0	323.15	97.2 (±0.4)	1.3 (±0.1)	2700 (±200)

The leaching solution used is from a molybdenum mine. c_{Re} is 90–100 mg/L, c_{Mo} is 62–65 g/L, and the amount of free ammonia is 80–100 g/L. After the whole leaching solution was diluted tenfold, the separation of Re (VII) and Mo (VI) in a simulated solution with 0.01 g/L of Re (VII), 6 g/L of Mo (VI), and 8 g/L of free ammonia was investigated under the suitable conditions. As shown in Table 4, E_{Re} reached 99.1%, and the $S_{Re/Mo}$ was 5100, confirming the efficient separation of Re (VII) and Mo (VI). In comparison to the methods proposed in Salehi et al.'s study [12] and Aifei Yi et al.'s study [4], this method not only has a high extraction efficiency but also a much higher separation factor than those in the cited studies.

Table 4. Separation results for Re (VII) and Mo (VI) in simulated leaching solution.

$c_{E\text{-}1006}$/ g L^{-1}	$c_{(NH4)2SO4}$/ g L^{-1}	pH	Temperature/ K	E_{Re}/%	E_{Mo}/%	$S_{Re/Mo}$
200	200	7.0	323.15	99.1 (±0.1)	2.1 (±0.2)	5100 (±400)

4. Conclusions

(1) A phase equilibrium diagram of the ATPS, composed of E-1006, $(NH_4)_2SO_4$, and water, was developed.

(2) The effects of pH, temperature, concentrations of ATPS components, and metal ions on the separation of Re (VII) and Mo (VI) were investigated. The results show that pH plays an important role in the separation of Re (VII) and Mo (VI). At pH 7.0, Mo (VI) almost transitioned into the $(NH_4)_2SO_4$-rich phase, while Re (VII) was extracted into the E-1006-rich phase, and the separation factor of Re (VII) and Mo (VI) reached a maximum of 129.67. The extraction efficiency of Re (VII) is higher at low temperatures. The increase in temperature promotes the transition of Mo (VI) to the salt-rich phase, and the separation factor of Re (VII) and Mo (VI) reaches a maximum of 139.37 at 323.15 K. The separation of Re (VII) and Mo (VI) is favored by increasing the concentrations of E-1006 and $(NH_4)_2SO_4$. An increase in the Re (VII) concentration decreases the extraction efficiency of Re (VII). An increase in the Mo (VII) concentration promotes the extraction of Re (VII) and Re-Mo separation.

(3) The suitable conditions for the separation of Re (VII) and Mo (VI) were achieved using an ATPS composed of 200 g/L of E-1006, 200 g/L of $(NH_4)_2SO_4$, and water at a pH 7.0 heated to 323.15 K for 2 h. A mixed solution of 0.1 g/L of Re (VII) and 5 g/L of Mo (VI) was separated by the ATPS. The extraction efficiency of Re (VII) reached 97.2%, and the separation factor of Re (VII) and Mo (VI) reached 2700. A diluted simulated leaching solution consisting of 0.1 g/L of Re and 5 g/L of Mo was separated using the ATPS. The extraction efficiency of Re (VII) reached 99.1%, and the separation factor of Re (VII) and Mo (VI) reached 5100.

Supplementary Materials: The following supporting information can be downloaded at: https://www.mdpi.com/article/10.3390/separations11050142/s1, Table S1. Phase equilibrium data for the ATPS of E-1006 and $(NH_4)_2SO_4$ at different temperature.

Author Contributions: L.F.: methodology, formal analysis, investigation, data curation, and writing—original draft. W.L.: investigation and writing—review and editing. Z.D.: formal analysis and investigation. M.Z.: investigation and data curation. Y.Q.: conceptualization, writing—review and editing, funding acquisition, and supervision. All authors have read and agreed to the published version of the manuscript.

Funding: This research was funded by the National Key R&D Program of China, grant number 2022YFC2904602, and the Fundamental Research Funds for the Central Universities of Central South University, grant number 2023ZZTS0737).

Data Availability Statement: The data that support the findings of this study are available from the corresponding author upon reasonable request.

Conflicts of Interest: The authors declare no conflicts of interest.

References

1. Xu, W.; Wang, W.; Chen, S.; Zhang, R.; Wang, Y.; Zhang, Q.; Yuwen, L.; Yang, W.J.; Wang, L. Molybdenum disulfide (MoS_2) nanosheets-based hydrogels with light-triggered self-healing property for flexible sensors. *J. Colloid Interface Sci.* **2020**, *586*, 601–612. [CrossRef] [PubMed]
2. Liu, B.; Zhang, B.; Han, G.; Wang, M.; Huang, Y.; Su, S.; Xue, Y.; Wang, Y. Clean separation and purification for strategic metals of molybdenum and rhenium from minerals and waste alloy scraps—A review. *Resour. Conserv. Recycl.* **2022**, *181*, 106232. [CrossRef]
3. Hori, H.; Yonezato, Y.; Ito, K. Recovery of platinum and rhenium using selective precipitation induced by two-stage photochemical treatment. *Hydrometallurgy* **2022**, *211*, 105883. [CrossRef]
4. Yi, A.; Jiang, H. Rhenium-molybdenum separation in an alkaline leaching solution of a waste superalloy by N263 extraction. *Arab. J. Chem.* **2023**, *16*, 104516. [CrossRef]
5. Wang, Q.; Wang, S.; Ma, X.; Cao, Z.; Zhang, C.; Zhong, H. A green production process of electrolytic manganese metal based on solvent extraction. *Colloids Surf. A Physicochem. Eng. Asp.* **2023**, *670*, 131517. [CrossRef]
6. Joo, S.-H.; Kim, Y.-U.; Kang, J.-G.; Kumar, J.R.; Yoon, H.-S.; Parhi, P.K.; Shin, S.M. Recovery of Rhenium and Molybdenum from Molybdenite Roasting Dust Leaching Solution by Ion Exchange Resins. *Mater. Trans.* **2012**, *53*, 2034–2037. [CrossRef]
7. Feng, J.; Li, J.; Liao, Y.; Liu, F.; Li, H.; Jiang, Q.; Huang, B.; Wang, Y.; Xiao, L.; Liu, H.; et al. Rhenium recovery from roasting leachate of molybdenum concentrate by N-methylimidazole functionalized anion exchange resin. *J. Radioanal. Nucl. Chem.* **2023**, *332*, 747–760. [CrossRef]
8. Fu, Z.; Hou, Y.; Huang, J.; Cheng, D.; Li, G. Separation and recovery of rhenium(VII) from molybdenum concentrate oxygen pressure leach solution by modified D201 resin. *Conserv. Util. Miner. Resour.* **2022**, *42*, 115–122.
9. Wang, J.; Yu, Z.; Xiao, X. A novel hydroxyapatite super-hydrophilic membrane for efficient separation of oil-water emulsions, desalting and removal of metal ions. *Desalination Int. J. Sci. Technol. Desalt. Water Purif.* **2023**, *565*, 116864. [CrossRef]
10. Long, X.; Zhao, G.Q.; Zheng, Y.; Hu, J.; Zuo, Y.; Luo, W.; Jiao, F. A precise pyromellitic acid grafting prepared multifunctional MXene membranes for efficient oil-in-water emulsion separation and heavy metal ions removal. *Chem. Eng. J.* **2023**, *472*, 144904. [CrossRef]
11. Kang, S.; Qin, S.-J.; Wang, Q.; Hao, L.; Pang, W.; Li, S. Research Progress on Separation Enrichment and Extraction Techology of Rhenium. *Nonferrous Met. Smelt. Compon.* **2023**, 66–74.
12. Salehi, H.; Tavakoli, H.; Aboutalebi, M.R.; Samim, H.R. Recovery of molybdenum and rhenium in scrub liquors of fumes and dusts from roasting molybdenite concentrates. *Hydrometallurgy* **2019**, *185*, 142–148. [CrossRef]
13. Kim, H.S.; Park, J.S.; Seo, S.Y.; Tran, T.; Kim, M.J. Recovery of rhenium from a molybdenite roaster fume as high purity ammonium perrhenate. *Hydrometallurgy* **2015**, *156*, 158–164. [CrossRef]
14. Srivastava, R.R.; Kim, M.; Lee, J.; Ilyas, S. Liquid–liquid extraction of rhenium(VII) from an acidic chloride solution using Cyanex 923. *Hydrometallurgy* **2015**, *157*, 33–38. [CrossRef]
15. Hong, T.; Liu, M.; Ma, J.; Yang, G.; Li, L.; Mumford, K.A.; Stevens, G.W. Selective recovery of Rhenium from industrial leach solutions by synergistic solvent extraction. *Sep. Purif. Technol.* **2020**, *236*, 116281. [CrossRef]
16. Assis, R.C.; Mageste, A.B.; de Lemos, L.R.; Orlando, R.M.; Rodrigues, G.D. Application of aqueous two-phase system for selective extraction and clean-up of emerging contaminants from aqueous matrices. *Talanta* **2021**, *223*, 121697. [CrossRef] [PubMed]
17. Zhang, F.; Jia, A.; Guo, Q.; Sun, T.; Li, P.; Wang, P.; Pan, Y.; Zhang, Y. Mass transfer of molybdenum in L35 + sodium sulfate + H_2O aqueous two-phase system with a packed column. *Sep. Purif. Technol.* **2018**, *204*, 304–313. [CrossRef]
18. Pan, Y.; Sun, X.; Qi, M.; Qin, R.; Che, X.; Zhang, Y. A clean and efficient method for separation of vanadium and molybdenum by aqueous two-phase systems. *J. Mol. Liq.* **2020**, *313*, 113540. [CrossRef]
19. Huang, Y.; Chen, D.; Chen, S.; Su, M.; Chen, Y.; Yuvaraja, G. A green method for recovery of thallium and uranium from wastewater using polyethylene glycol and ammonium sulfate based on aqueous two-phase system. *J. Clean. Prod.* **2021**, *297*, 126452. [CrossRef]
20. Li, R.; Qin, R.; Li, Q.; Zhang, Y.; Zhang, Y. Study on extraction and separation of tungsten and molybdenum by nonionic surfactant Triton X-100/Na_2SO_4 two-phase aqueous system. *Chem. World* **2023**, *64*, 342–347. [CrossRef]
21. Leite, D.D.S.; Carvalho, P.L.G.; De Lemos, L.R.; Mageste, A.B.; Rodrigues, G.D. Hydrometallurgical separation of copper and cobalt from lithium-ion batteries using aqueous two-phase systems. *Hydrometallurgy* **2017**, *169*, 245–252. [CrossRef]
22. García-González, L.; Shirayama, S.; Morita, K. Cobalt and nickel separation in aqueous two-phase systems with polyethylene glycol 20,000 and sodium electrolytes. *Hydrometallurgy* **2023**, *222*, 106180. [CrossRef]
23. Hishida, M.; Kaneko, Y.; Yamamura, Y.; Saito, K. Salt Effects on Lamellar Structure of Nonionic Surfactants. *J. Solut. Chem.* **2016**, *45*, 1612–1619. [CrossRef]
24. Lindman, B.; Medronho, B.; Karlström, G. Clouding of nonionic surfactants. *Curr. Opin. Colloid Interface Sci.* **2016**, *22*, 23–29. [CrossRef]
25. Guedes De Carvalho, R.A.; Sampaio, M.N.M. Solvent extraction of tungsten by alkylamines hydrochloric acid and alkylamines-sulphuric acid systems. *Hydrometallurgy* **1991**, *26*, 137–150. [CrossRef]
26. Fei, Y.; Gou, S.; He, Y.; Zhou, L.; Peng, C.; Zhang, H.; Zhang, Q.; Wu, Y. The properties of polyoxyethylene polymers with temperature-sensitive and instant-solubility. *J. Mol. Liq.* **2019**, *275*, 146–156. [CrossRef]

27. Tang, Z.; Wang, H.; Wu, P.-F.; Zhou, S.-Y.; Huang, Y.-C.; Zhang, R.; Sun, D.; Tang, Y.-G.; Wang, H.-Y. Electrode–Electrolyte Interfacial Chemistry Modulation for Ultra-High Rate Sodium-Ion Batteries. *Angew. Chem. Int. Ed.* **2022**, *61*, e202200475. [CrossRef] [PubMed]
28. Vasylieva, A.; Doroshenko, I.; Vaskivskyi, Y.; Chernolevska, Y.; Pogorelov, V. FTIR study of condensed water structure. *J. Mol. Struct.* **2018**, *1167*, 232–238. [CrossRef]
29. Han, D.; Li, X.; Cui, Y.; Yang, X.; Chen, X.; Xu, L.; Peng, J.; Li, J.; Zhai, M. Polymeric ionic liquid gels composed of hydrophilic and hydrophobic units for high adsorption selectivity of perrhenate. *RSC Adv.* **2018**, *8*, 9011–9319. [CrossRef]
30. Zhang, Y.; Sun, T.; Hou, Q.; Guo, Q.; Lu, T.; Guo, Y.; Yan, C. A green method for extracting molybdenum (VI) from aqueous solution with aqueous two-phase system without any extractant. *Sep. Purif. Technol.* **2016**, *169*, 151–157. [CrossRef]
31. Ahsaie, F.G.; Pazuki, G. Effect of carbohydrates, choline chloride based deep eutectic solvents and salts on the phase behavior of PEG-PPG copolymer ATPSs and partitioning of penicillin G. *J. Mol. Liq.* **2021**, *339*, 117152. [CrossRef]
32. Sinoimeri, E.; Pescheux, A.-C.; Guillotte, I.; Cognard, J.; Svecova, L.; Billard, I. Fate of metal ions in PEG-400/Na_2SO_4/H_2O aqueous biphasic system: From eviction to extraction towards the upper polymer-rich phase. *Sep. Purif. Technol.* **2023**, *308*, 122854. [CrossRef]
33. Jin, L.; Jarand, C.W.; Brader, M.L.; Reed, W.F. Angle-dependent effects in DLS measurements of polydisperse particles. *Meas. Sci. Technol.* **2022**, *33*, 045202. [CrossRef]
34. Akach, J.; Kabuba, J.; Ochieng, A. Simulation of the Light Distribution in a Solar Photocatalytic Bubble Column Reactor Using the Monte Carlo Method. *Ind. Eng. Chem. Res.* **2020**, *59*, 17708–17719. [CrossRef]
35. Lou, Z.; Guo, C.; Feng, X.; Zhang, S.; Xing, Z.; Shan, W.; Xiong, Y. Selective extraction and separation of Re(VII) from Mo(VI) by TritonX-100/N235/iso-amyl alcohol/n-heptane/NaCl microemulsion system. *Hydrometallurgy* **2015**, *157*, 199–206. [CrossRef]
36. Boysen, R.I.; Wang, Y.; Keah, H.H.; Hearn, M.T. Observations on the origin of the non-linear van't Hoff behaviour of polypeptides in hydrophobic environments. *Biophys. Chem.* **1999**, *77*, 79–97. [CrossRef]